Mechanism and Optimization of Metal Deposition onto Vertically Aligned Single-Walled Carbon Nanotube Arrays

Hai M. Duong, Kei Ishikawa, Jun Okawa, Kazuaki Ogura, Erik Einarsson, Junichiro Shiomi, and Shigeo Maruyama*

Department of Mechanical Engineering, The University of Tokyo, 7-3-1 Hongo, Bunkyo-ku, Tokyo 113-8656, Japan

Received: March 25, 2009; Revised Manuscript Received: May 19, 2009

Arrays of vertically aligned single-walled carbon nanotubes (VASWNTs) were coated with thin films of Ti, Pd, Au, and Al by evaporative deposition. Scanning electron microcopy showed the Ti and Pd coatings were continuous or quasi-continuous, whereas Au and Al agglomerated into discrete deposits on SWNT bundles. The mechanism of metal film formation on VASWNT arrays was studied by observing the film at various stages of the deposition process. Uniformity of the deposition was found to be strongly dependent on the metal species and the deposition conditions, such as substrate temperature, deposition rate, and deposition thickness. The optimization of the deposition conditions was demonstrated for Pd. The results suggest that the deposition efficiency for a smooth coating layer is determined by the balance of two processes with significantly different speeds: the coating along an SWNT bundle and coating of an interbundle, which depend on the metal type and the deposition conditions. These findings may be useful regarding both fundamental and practical aspects of VASWNT applications in thermal and electronic devices.

1. Introduction

Single-walled carbon nanotubes (SWNTs)[1,2] have attracted much attention as promising materials for next-generation thermal and electrical devices because of their extraordinary thermal and electrical properties.[3,4] Although possibilities for single-channel devices with an individual SWNT[5] have been extensively explored, bulk SWNT materials in the form of mats and films are expected to play an important role in the near future applications due to their handling and cost efficiencies. Among the bulk SWNT materials, vertically aligned SWNT (VASWNT) arrays[6−12] have attracted great attention to realize directional bulk transport devices. Particularly, the VASWNTs grown by the alcohol catalytic CVD method[6,13−15] are known to have high crystallinity. Furthermore, the synthesized films consist of very small bundles separated by large interbundle distances; thus, the films retain, to some extent, properties of individual SWNTs.

Regarding device applications of VASWNT film as thermal and electrical devices, metal film coating is an important element technology for integration and probing intrinsic properties. Here, studying the metal−SWNT interaction is a primary issue as the contact resistance significantly influences the performance and the electrical/thermal conductance in the large mean-free-path systems. Reports on the strong dependence of carbon nanotube transport characteristics on metal type[17,18] have motivated vacuum-evaporation experiments for various metals and deposition conditions,[19] which revealed strongly metal-dependent morphologies.

The metal deposition on the individually suspended SWNTs was investigated by Zhang et al.,[19] who coated various metals onto individually suspended SWNTs by electron-beam evaporation and observed the metal morphologies using transmission electron microscopy. It was shown that Ti exhibited better coverage than that of Au and Al, which was consistent with the interfacial resistances obtained in the transport measurements.[17,18] The metal-dependent nucleation was explained by the surface diffusion rate of adatoms, where the activation energy can be empirically related to the binding energy for the smooth coating surface of an individual SWNT. From the observed nucleation densities and size of the formed clusters, they have predicted high metal−SWNT binding energies for Ti and Pd, which agrees with a later numerical study.[20]

Although the early growth process of the metal layer deposited onto a VASWNT film can be understood from the coating of the individual SWNTs, the full coating process is expected to be much more complicated due to the three-dimensional nanostructured surface of the VASWNT film and the multistage nature of the metal-layer formation. When metal is deposited on top of a VASWNT film, each SWNT bundle becomes a nucleation site to form grains along the SWNT. Although the coalescence of grains leads to the formation of a continuous metal layer as in usual metal deposition onto a planar substrate,[21] the morphology of the VASWNT limits interbundle metal mass transfer by surface diffusion. This results in two events with significantly different time scales: fast intrabundle coalescence of clusters by surface diffusion, resulting in larger grains, and slow interbundle coalescence that requires further growth of the grains and intrabundle mass transport. These anisotropic and multi-timescale coalescence processes are expected to strongly influence the final smoothness and filling ratio of the metal layer.

In this work, the formation mechanism and resulting structures of four different kinds of VASWNT−metal (Au, Al, Ti, and Pd) films were systematically investigated. The smoothness of the VASWNT−metal films depended strongly on the metal species, substrate temperature, deposition rate, and thickness of the deposited metal layer. This leads us to identify the optimized conditions for obtaining the smooth and uniform metal coating on the VASWNT films.

* Corresponding author. E-mail: maruyama@photon.t.u-tokyo.ac.jp. Phone: +81-3-5841-6421. Fax: +81-3-5800-6985.

10.1021/jp902708k CCC: $40.75
Published on Web 07/15/2009

2. Experimental Section

2.1. VASWNT Synthesis. VASWNTs were synthesized on quartz substrates using the alcohol catalytic chemical vapor deposition (ACCVD) process.[6,13−15] The catalyst was supported on a quartz substrate, which was dip-coated into a Co−Mo acetate solution (metal content, 0.01 wt % each, dissolved in ethanol). The catalyst was oxidized by heating the dip-coated substrate in air at 400 °C and then reduced in a flowing Ar/H_2 mixture (3% H_2, 300 sccm flow rate, 40 kPa) during heating of the growth chamber. When the SWNT growth chamber reached 800 °C, the Ar/H_2 flow was stopped and SWNTs were synthesized by supplying ethanol vapor at 1.3 kPa (10 Torr) until the VASWNT array had reached approximately 5 μm in thickness. The average diameter of the VASWNTs was 1.9 nm.[6]

2.2. Deposition and Characterization of Metal Films. An evaporative deposition chamber (ULVAC VPC-260F) was used for metal deposition, and characterization was primarily done by SEM observation (JEOL JSM-7000F). Thin films of Au, Al, Ti, and Pd were deposited onto the VASWNT arrays. The deposition rate and thickness of the deposited films were determined using the built-in quartz crystal microbalance, which was calibrated using flat substrates. Because the VASWNT arrays are very porous, it is difficult to define the thickness of the deposited film. Thus, we use the "nominal" film thickness to indicate the thickness of a metal film if it had been deposited onto an atomically flat surface. A resistively heated target holder allowed the substrate temperature to be controlled between room temperature (approximately 25 °C) and 300 °C. Unless otherwise indicated, the VASWNT target is at room temperature during deposition.

3. Results and Discussion

3.1. Interactions of Metals and Bundled SWNTs. To study the initial stage of the metal deposition and the interactions of the metal adatoms with the SWNTs, 4 nm films of each of the four metal species (Au, Al, Ti, and Pd) were deposited onto the VASWNT arrays with a deposition rate of 0.05 nm/s. The resulting morphologies are shown in the SEM images in Figure 1. Au and Al (Figure 1a,b) formed discrete clusters on the SWNT bundles, leaving some areas free of metal coating. The observation indicates that Au and Al adatoms deposited on the SWNT bundles have diffused along the bundle surface and agglomerated into larger clusters. This suggests a small activation energy for surface diffusion of Au and Al adatoms on the SWNT surface, which agrees with the small binding energy of Au− and Al−SWNTs.[20] Figure 1d shows the deposition of Ti, which formed a continuous and uniform coating on SWNTs. The deposition of Pd (Figure 1c) resulted in semi-uniform coverage, with some discontinuous areas. The deposited Ti and Pd appear as small clusters, smoothly connected together along the SWNT bundles. These results are consistent with the work of Zhang et al.,[19] showing that Ti adatoms exhibit a higher continuity than that of Pd and much higher than that of Au and Al, reflecting the order of binding energy to an SWNT.[20]

The binding energy of individual metal atoms (Au, Al, Pd, and Ti) adsorbed on a (8,0) zigzag SWNT and a (6,6) armchair SWNT has been calculated by using the pseudopotential plane wave methods within the generalized gradient approximation.[20] For instance, for the (8,0) SWNT case without spin polarization, they obtained binding energies of 0.6, 1.6, 2.7, and 2.9 eV for Au, Al, Pd, and Ti, respectively. The good correlation between the order of binding energy and the observed metal-dependent cluster size implies a major role of binding energy on determining the film morphologies. Note that quantitative comparison with the above numerical simulations would require further investigations on the curvature effect because the binding energy of an adatom adsorbed on an SWNT has been reported to decrease with increasing nanotube diameter and eventually saturate at a value of that on a graphene.[22]

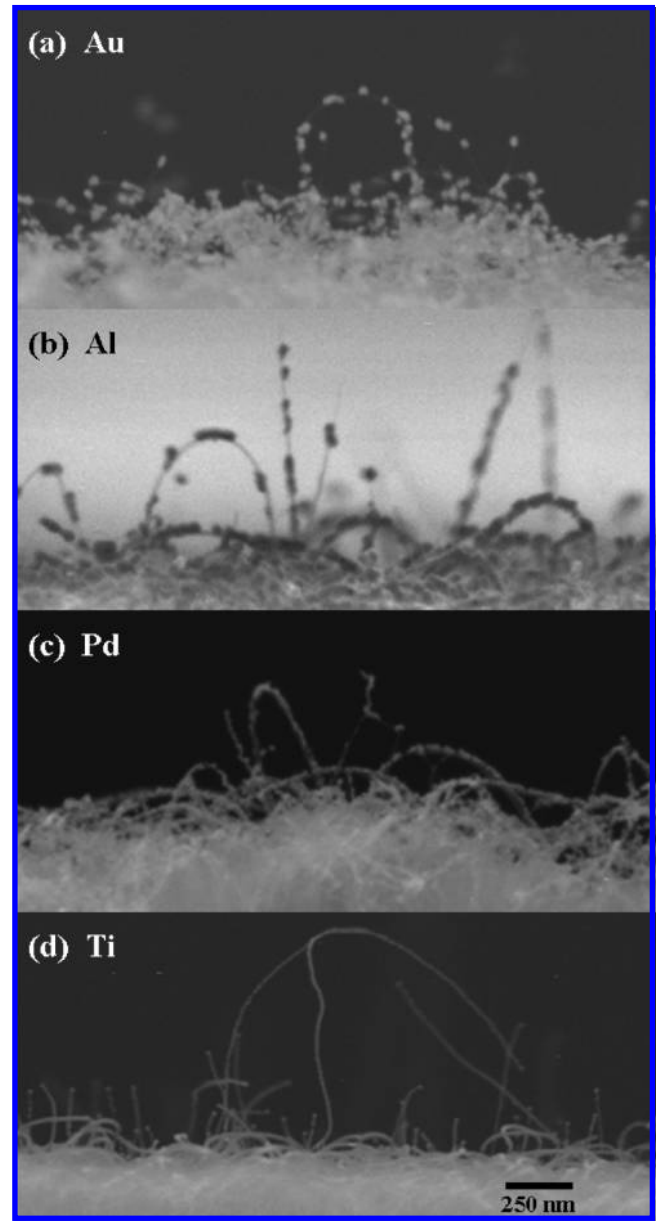

Figure 1. SEM images of VASWNTs coated with a 4 nm layer of (a) Au, (b) Al, (c) Pd, and (d) Ti. The deposition rate was 0.05 nm/s, and the substrate temperature was 25 °C.

3.2. Coating Mechanisms of Metal Film Formation on SWNT Arrays. To study the coating scenario, Pd films with nominal thicknesses of 4, 10, 25, 50, 100, and 200 nm were deposited onto the VASWNT arrays. The substrate temperature was 25 °C. The deposition rates were 0.05 nm/s for the 4 nm film and 0.20 nm/s for the thicker films. SEM images of the resulting morphologies are shown in Figure 2a−f (in order of increasing thickness). As can be seen in Figure 2a, initially, the Pd adatoms form a uniform coating of fine clusters on the SWNT bundles, with some discontinuous regions. Although we cannot identify with the current investigation, the nucleation sites are expected to be located at the bundle grooves with high interfacial potential energy. As deposition continues (Figure

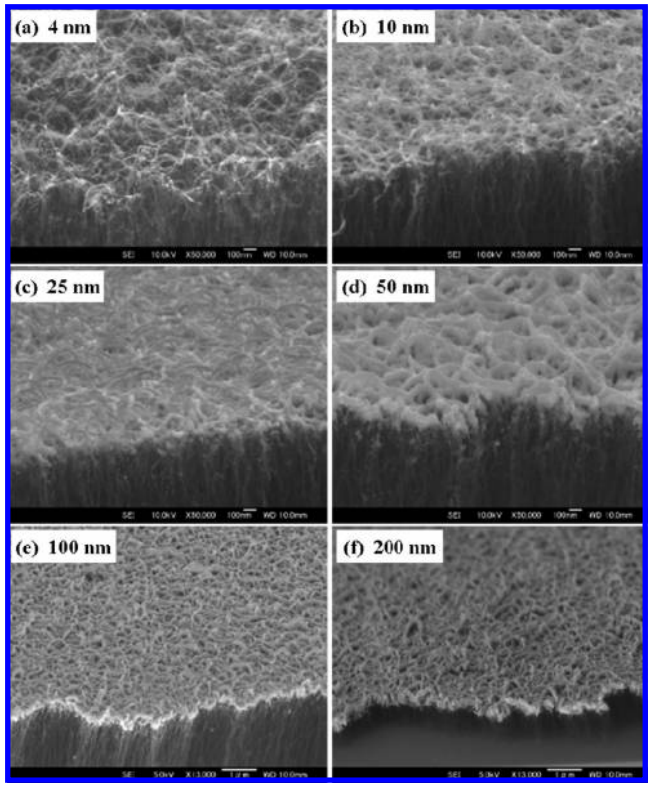

Figure 2. SEM images of VASWNTs coated with Pd films (a) 4 nm, (b) 10 nm, (c) 25 nm, (d) 50 nm, (e) 100 nm, and (f) 200 nm thick. The deposition rate was 0.20 nm/s, and the substrate temperature was 25 °C.

2b,c), the nucleation sites on the top SWNT layer rapidly approach a saturation density, and then additional Pd adatoms fill in the gaps between nucleation sites along SWNTs. This results in uniform coating of the SWNTs on the top layer with the coating thickness growing with the amount of deposited metal. Note that, at this diffusion-controlled stage, the diffusion dominantly takes place along an SWNT bundle because the film morphology limits the interbundle mass transport.

The initial growth of clusters along an SWNT bundle leads to the formation of larger scale grains by surface diffusion of adatoms and small clusters. As the grain sizes increase with further metal deposition and become larger than the distances between the coated SWNT bundles, the grains begin to coalesce. The rate of increase in the grain size and corresponding decrease in the grain density are influenced by the deposition condition, as discussed later. The coalescence of grains opens mass transport channels among the grains and forms larger network structures of "islands". Unlike the coalescence of metal islands on a planar surface, where a rapid large-scale coalescence of the metal clusters takes place when the island density reaches a critical state,[21] the coalescence is expected to take place relatively slowly in the current case due to lack of interbundle mass transfer. The island coalescence leaves empty channels,[21] as shown in Figure 2d. The channels can be filled with the addition of deposition (Figure 2d−f), but the process of the adatoms filling in the empty channels is slow[21] and requires a considerable amount of Pd adatom deposit, particularly for the current "nanopore" system.

The resulting morphology of the metal layer after deposition of a 100 nm nominal thickness clearly depends on the metal type, as shown in Figure 3. The deposition rate was 0.20 nm/s for all the cases. The grains of Ti and Pt films (Figure 3a,b) are elongated along the underlying SWNT bundles, whereas those

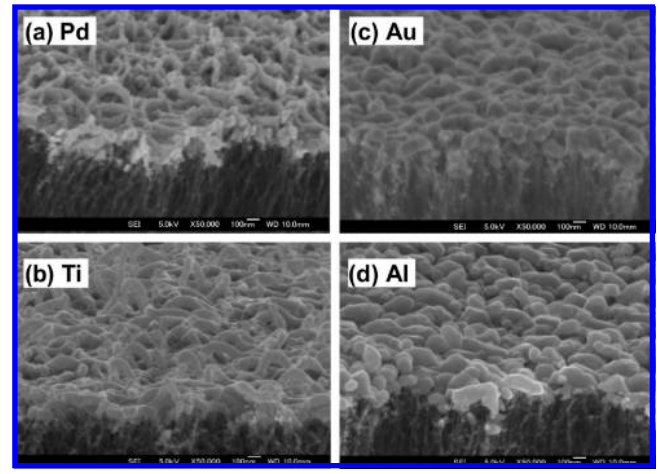

Figure 3. SEM images of different VASWNTs coated with a 100 nm layer of (a) Pd, (b) Ti, (c) Au, and (d) Al. The deposition rate was 0.20 nm/s, and the substrate temperature was 25 °C.

TABLE 1: Summary of Deposition Conditions

metals	nominal thickness (nm)	coating rate (nm/s)	substrate temperature (°C)
		Section 3.1	
Au	4.0	0.05	25
Al	4.0	0.05	25
Ti	4.0	0.05	25
Pd	4.0	0.05	25
		Section 3.2	
Pd	4	0.05	25
Pd	10	0.20	25
Pd	25	0.20	25
Pd	50	0.20	25
Pd	100	0.20	25
Pd	200	0.20	25
		Section 3.3	
Au	100	0.20	25
Au	100	0.20	300
Al	100	0.20	25
Al	100	0.20	300
Ti	100	0.20	25
Ti	100	0.20	300
Pd	100	0.20	25
Pd	100	0.20	300
Pd	100	0.05	25
	100	0.20	25
	100	0.40	25
Pd	50	0.20	25
	100	0.20	25
	200	0.20	25

of the Au and Al films (Figure 3c,d) were largely spheroid clusters, inheriting the characteristics of the initial cluster nucleation (Figure 1). Although Au and Al clusters exhibit relatively more frequent interbundle bridging with larger grains, they also create more empty channels, which take a significantly greater amount of deposition to fill and achieve a smooth film. On the other hand, in the cases of Ti and Pd, the continuous coverage of individual SWNT bundles results in more planar film.

3.3. Optimization of the Parameters of the Coating Process of the SWNT−Metal Films. The smoothness of the SWNT−metal films depended not only on the coated metal types but also on all three experimental parameters: substrate temperature, deposition rate, and metal thickness. To find the optimal coating conditions, one of these parameters was changed while two others were kept constant. The effects of the coating parameters on the smoothness of the SWNT−metal films were

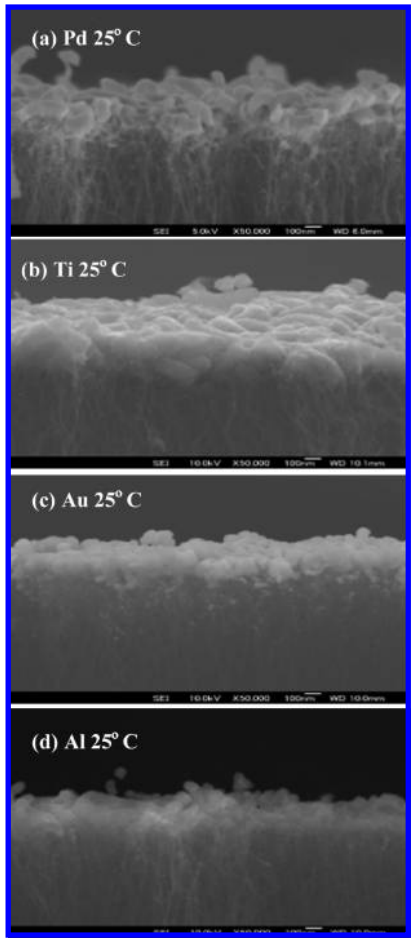

Figure 4. SEM images showing cross sections of VASWNT−metal films from Figure 3. Films are 100 nm thick (a) Pd, (b) Ti, (c) Au, and (d) Al.

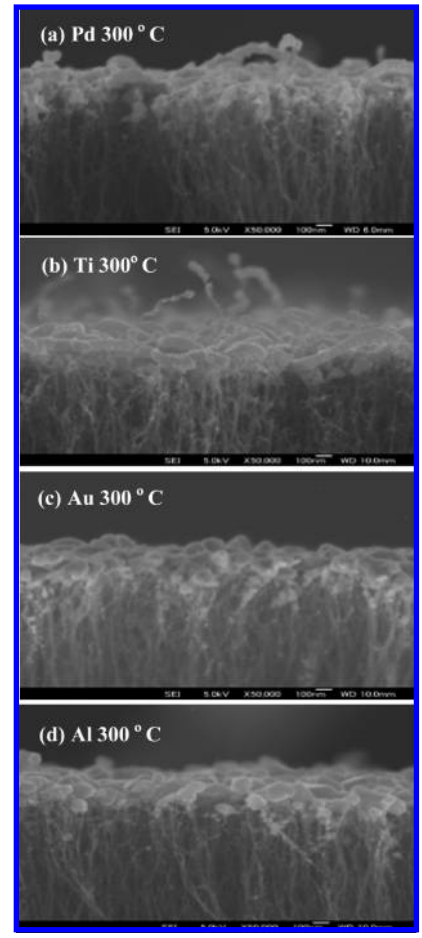

Figure 5. SEM images showing cross sections of VASWNT−metal films deposited with the substrate heated to 300 °C. Film thicknesses are 100 nm of (a) Pd, (b) Ti, (c) Au, and (d) Al, deposited at 0.20 nm/s.

studied by coating Pd onto SWNT arrays synthesized under the same CVD conditions.

3.3.1. Effect of Substrate Temperature. The role of substrate temperature was investigated by depositing 100 nm of Au, Al, Ti, and Pd at 25 and 300 °C. The deposition rate was 0.20 nm/s for all the cases (Table 1). Cross-sectional SEM images of the SWNT−Pd, −Ti, −Au, and −Al films deposited at room temperature are shown in Figure 4a−d and those deposited at 300 °C in Figure 5a−d. At higher substrate temperature, the surface mobility of adatoms increases. Whereas in the initial "intrabundle coating" stage, this decreases the nucleation density and increases the cluster size, in the later "interbundle coating" stage, it makes the condensation occur more preferentially at the surface concaves.[21] As a result, the surfaces of the SWNT−metal films are smoother when deposited at 300 °C, as seen in Figure 5a−d. Although temperature promotes the film smoothness by enhancing the interbundle metal mass transport, excess temperature is expected to decrease the nucleation density and increase the size of clusters at the initial stage and results in more interbundle empty channels. In addition, increasing the temperature allows metal adatoms to penetrate deeper into the SWNT arrays and stick along the SWNT bundles. These suggest that, to efficiently achieve a smooth and uniform metal layer, there exists an optimal window of temperature, which should depend on the metal type, reflecting the differences in interfacial binding energy and cohesive energy.

3.3.2. Effect of Deposition Rate. To study the effect of the deposition rate on the film smoothness and uniformity, we coated the same amount (100 nm) of Pd onto VASWNT arrays with different coating rates. The resulting films are shown by cross-sectional SEM images in Figure 6a−c, where the metal was deposited at room temperature using rates of 0.05, 0.20, and 0.40 nm/s, respectively. The figure shows that the grain size is the largest for the 0.20 m/s case and the film is smoothest for the 0.40 m/s case. Note that the visual film thickness is smallest for the highest deposition rate case (0.40 m/s), which suggests the highest filling ratio of the interbundle spacing. The results indicate important roles of kinetic energy of the adatoms on the obtained final film morphology. The higher deposition rate gives larger kinetic energy, which first, enhances the surface mobility and, thus, results in larger clusters in the initial growth along the nanotube bundle. When the deposition rate is high enough (0.40 m/s), for the given deposition thickness, the kinetic energy enhances the interbundle metal mass transfer and, therefore, the interbundle grain coalescence becomes faster, resulting in a smoother metal film. In this context, the deposition ratio has a similar effect as the previously discussed temperature effect.

Higher deposition rate is also often related to lower diffusion rate due to the stronger binding with the substrate, which would result in more nucleation sites and, thus, smaller-size clusters. However, the current result shows the opposite trend, which suggests that the current range of deposition rates is sufficiently smaller than the relaxation rate to thermodynamic equilibrium.

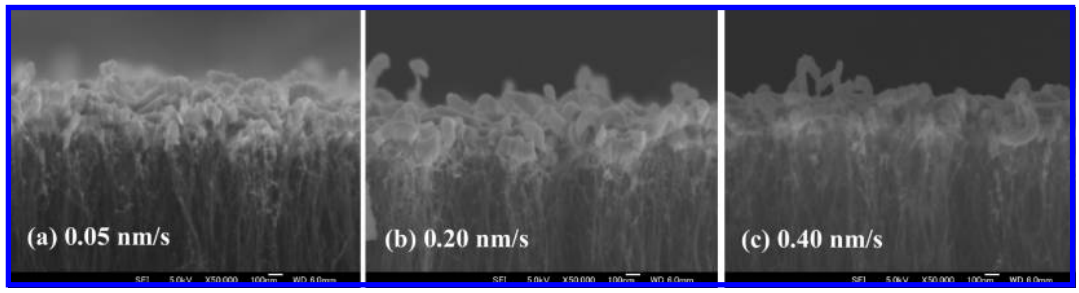

Figure 6. SEM images observed on the side of the SWNT−Pd films with a 100 nm Pd thickness coated at room temperature at different metal coating rates: (a) 0.05 nm/s, (b) 0.20 nm/s, and (c) 0.40 nm/s.

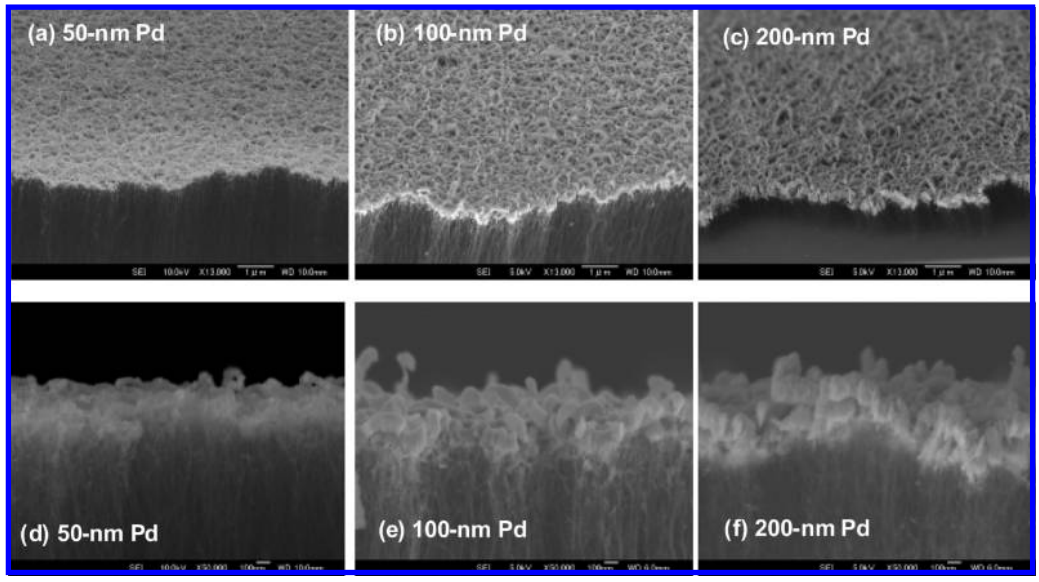

Figure 7. SEM images of the top and side of VASWNT−Pd films. Pd thicknesses are (a, d) 50 nm, (b, e) 100 nm, and (c, f) 200 nm. The deposition rate was 0.20 nm/s, and the substrate temperature was 25 °C.

3.3.3. Effect of the Metal Thickness on the SWNT−Metal Films. The effect of the metal thickness on film smoothness was studied by depositing 50, 100, and 200 nm thick Pd films on top of VASWNT arrays. The deposition rate was 0.20 nm/s, and the substrate temperature was 25 °C. Top-view and cross-sectional SEM images of SWNT−Pd films with thicknesses of 50, 100, and 200 nm are shown in Figure 7a−c (top) and Figure 7d−f (side), respectively. In Figure 7a,d, a coating thickness of 50 nm of Pd is not sufficient to fill in the empty spaces in the SWNT−Pd films. When more Pd is deposited, the empty channels are mostly filled (Figure 7b), and larger Pd islands are formed on the top of the array (Figure 7e). Figure 6f shows that, with a thicker Pd layer, cubic Pd particles are formed, resulting in a smooth surface of 200 nm thick SWNT−Pd film. For low-resistance contact, it is important that the internal empty channels are filled. The result shows, for Pd deposition at room temperature and a realistic range of deposition rates, an unusually thick deposition thickness of about 200 nm is required to achieve a smooth surface. Although this is usually a very slow process involving internal mass diffusion rather than the fast surface diffusion, the current nanopore system with limited interbundle mass transport is expected to require even more time and deposition for the internal film structure to saturate.

4. Conclusions

Thin films of four different metals (Au, Al, Ti, and Pd) were deposited onto the VASWNT arrays by an evaporative deposition method. When the various parameters were systematically adjusted, the growth process and morphologies of the thin metal films were investigated. Depending on the metal species, continuous films (for Ti and Pd) or discrete clusters (for Au and Al) formed on the SWNT bundles during the early stage of the coating process, reflecting the differences in the binding energy. In the later stage of the coating process, although Au and Al clusters exhibit faster interbundle bridging due to the growth of large grains, they also create more empty channels, which take a significantly greater amount of metal deposition to fill and achieve a uniform film. On the other hand, Ti and Pd with stronger binding energy show better coverage of an individual SWNT bundle, but the interbundle bridging takes place relatively slowly. Therefore, the deposition efficiency for a smooth coating layer is determined by the balance of the intrabundle and interbundle coating. We have identified the deposition parameter window, within a typical range in vacuum metal deposition, for Pd that efficiently realizes a smooth metal layer. The current results also provide guidelines to optimize the coating efficiency for other metal types.

References and Notes

(1) Iijima, S. *Nature* **1991**, *354*, 56.
(2) Iijima, S.; Ichihashi, T. *Nature* **1993**, *363*, 603.
(3) Dresselhaus, M. S.; Dresselhaus, G.; Eklund, P. C. *Science of Fullerenes and Carbon Nanotubes*; Academic Press: San Diego, CA, 1996.
(4) Jorio, A., Dresselhaus, G., Dresselhaus, M. S., Eds. *Carbon Nanotubes: Advanced Topics in the Synthesis, Structure, Properties and Applications*; Topics in Applied Physics 111; Springer-Verlag: New York, 2008.

(5) Tans, S. J.; Verschueren, A. R. M.; Dekker, C. *Nature* **1998**, *393*, 49.
(6) Murakami, Y.; Chiashi, S.; Miyauchi, Y.; Hu, M.; Ogura, M.; Okubo, T.; Maruyama, S. *Chem. Phys. Lett.* **2004**, *385*, 298.
(7) Hata, K.; Futaba, D. N.; Mizuno, K.; Namai, T.; Yumura, M.; Iijima, S. *Science* **2004**, *306*, 1362.
(8) Zhang, G.; Mann, D.; Zhang, L.; Javey, A.; Li, Y.; Yenilmez, E.; Wang, Q.; McVittie, J. P.; Nishi, Y.; Gibbons, J.; Dai, H. *Proc. Natl. Acad. Sci. U.S.A.* **2005**, *102*, 16141.
(9) Zhong, G.; Iwasaki, T.; Honda, K.; Furukawa, Y.; Ohdomari, I.; Kawarada, H. *Jpn. J. Appl. Phys.* **2005**, *44*, 1558.
(10) Eres, G.; Kinkhabwala, A. A.; Cui, H.; Geohegan, D. B.; Puretzky, A. A.; Lowndes, D. H. *J. Phys. Chem. B* **2005**, *109*, 16684.
(11) Xu, Y.-Q.; Flor, E.; Kim, M. J.; Hamadani, B.; Schmidt, H.; Smalley, R. E.; Hauge, R. H. *J. Am. Chem. Soc.* **2006**, *128*, 6560.
(12) Noda, S.; Hasegawa, K.; Sugime, H.; Kakehi, K.; Zhang, Z.; Maruyama, S.; Yamaguchi, Y. *Jpn. J. Appl. Phys.* **2007**, *46*, L399.
(13) Maruyama, S.; Kojima, R.; Miyauchi, Y.; Chiashi, S.; Kohno, M. *Chem. Phys. Lett.* **2002**, *360*, 229.
(14) Maruyama, S.; Einarsson, E.; Murakami, Y.; Edamura, T. *Chem. Phys. Lett.* **2005**, *403*, 320.
(15) Hu, M.; Murakami, Y.; Ogura, M.; Maruyama, S.; Okubo, T. *J. Catal.* **2004**, *225*, 230.
(16) Einarsson, E.; Shiozawa, H.; Kramberger, C.; Rümmeli, M. H.; Grüneis, A.; Pichler, T.; Maruyama, S. *J. Phys. Chem. C* **2007**, *111*, 17861.
(17) Dai, H.; Kong, J.; Zhou, C.; Franklin, N.; Tombler, T.; Cassell, A.; Fan, S.; Chapline, M. *J. Phys. Chem. B* **1999**, *103*, 11246.
(18) Zhou, C.; Kong, J.; Dai, H. *Phys. Rev. Lett.* **2000**, *84*, 5604.
(19) Zhang, Y.; Franklin, N. W.; Chen, R. J.; Dai, H. *Chem. Phys. Lett.* **2000**, *331*, 35.
(20) Durgun, E.; Dag, S.; Bagci, V. M.; Gulseren, O.; Yildirim, T.; Ciraci, S. *Phys. Rev. B* **2003**, *67*, 201401.
(21) Chopra, K. L. *Thin Film Phenomena*; R. E. Krieger Publishing Co.: Huntington, NY, 1979; p 137.
(22) Gulseren, O.; Yildirim, T.; Ciraci, S. *Phys. Rev. Lett.* **2001**, *87*, 116802.

JP902708K